Effects of Flux and Torque Hysteresis Band Amplitude in Direct Torque Control of Induction Machines

D. Casadei, G. Grandi, G. Serra, A. Tani

Istituto di Elettrotecnica, Università di Bologna, viale Risorgimento 2, 40136 Bologna - Italy
phone: +39-51-6443567; fax:+39-51-6443588; e-mail: gruppo_macc@eletb2.cineca.it

Abstract **- Direct torque control of induction machines allows high dynamic performance to be obtained utilising a simple signal processing method. Furthermore, this control technique doesn't require current regulators so reducing the hardware requirements. In this paper the influence of the amplitude of flux and torque hysteresis bands on switching frequency, torque and flux ripple, current distortion and drive losses is investigated. The advantages of a careful choice of hysteresis band amplitudes are emphasised. The numerical results are verified by experimental tests carried out on a DSP based processing system.**

Introduction

In recent years, control techniques for high-performance induction motor drives have been largely developed as alternative solutions to high-performance four-quadrant DC servo drives. Many schemes have been proposed, all based on the decoupling of flux and torque control variables. The flux and torque are estimated using various combinations of stator voltage, stator current, and shaft position or speed. The control variables are usually the stator current components, then current regulators are used to generate the appropriate gate signals to the inverter switches.

In Direct Torque Control (DTC) of induction machines the control strategy is based on selecting the proper voltage vector in order to maintain the torque and the stator flux within two hysteresis bands [1], [2]. In [3] and [4] a control method is presented in which the stator flux is guided to describe a hexagonal path in order to reduce the switching frequency. Both control schemes can be implemented utilising simple methods of signal processing without the need of current regulators, proportional-integral control of flux and torque and PWM pulse generation.

In previous papers [5], [6] a control scheme based on direct control of the torque has been proposed, which utilises as reference the rotor flux instead of stator flux. In this way it is possible to combine the advantages of rotor flux orientation and stator flux control without the need of determining the instantaneous position of the rotor flux. In particular, the highest pull-out torque is obtained and a change in rotor flux command is followed with a time constant which is much lower than that involved in stator current control. Furthermore, this approach has the advantage of requiring motor parameters which are moderately affected by saturation.

As previously described, the direct torque control of induction machine is based on the use of two hysteresis controllers. Small flux hysteresis bands lead to sinusoidal current waveforms, while small torque hysteresis bands allow smoothed torque to be generated. On the other hand, small hysteresis bands usually determine high switching frequency thereby increasing the switching losses.

This paper presents a detailed analysis on the effects of both flux and torque hysteresis band amplitudes on drive performance. In particular, the attention has been mainly focused on harmonic current distortion, average inverter switching frequency, torque pulsation and drive losses.

Decoupling Control of Torque and Flux

In order to obtain an accurate dynamic representation of the motor, it is necessary to base the calculation on the coupled circuit equations of induction machines. The equations, written in terms of d-q spatial vector and referred to a stator reference frame, are

$$\bar{v}_s = R_s \bar{i}_s + p\bar{\Phi}_s \quad (1)$$

$$0 = R_r \bar{i}_r + p\bar{\Phi}_r - jP\omega_m\bar{\Phi}_r \quad (2)$$

where

$$\bar{\Phi}_s = L_s \bar{i}_s + M\bar{i}_r \quad (3)$$

$$\bar{\Phi}_r = L_r \bar{i}_r + M\bar{i}_s \quad (4)$$

and

P	pole pairs
p	differential operator (d/dt)
s,r	subscripts for stator and rotor quantities
L,M	self and mutual inductance
R	winding resistance
ω_m	rotor angular speed

The electromagnetic torque can be expressed as

$$T = P\,\bar{i}_s \cdot j\bar{\Phi}_s \quad (5)$$

A block diagram representing the direct torque control scheme is shown in Fig. 1. The input commands of the control system are the desired stator flux magnitude Φ_s^* and torque T^*. The actual value of stator flux can be evaluated utilising the voltage model, the current model or a combination of them [7]

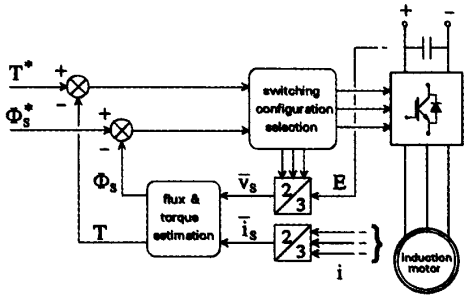

Fig. 1 - Block diagram of the DTC system.

0-7803-1328-3/94$03.00© 1994 IEEE

In Fig. 1 the switching configuration selection block determines the state of the inverter switches on the basis of the instantaneous errors in torque and flux.

In voltage source inverters eight switching combinations can be selected according to the following relationship

$$\bar{v}_s = \sqrt{\frac{2}{3}} E\left(S_a + S_b e^{j2\pi/3} + S_c e^{j4\pi/3}\right) \quad (6)$$

where

E = DC link voltage

S_a, S_b, S_c = inverter switching state

a,b,c = subscripts for phases.

Two switching combinations determine zero voltage vectors and the remaining generate six equally spaced vectors.

In general the selection of the proper voltage vector is made in order to maintain the torque and the stator flux within the limits of two hysteresis bands. From Eq. 1, assuming the voltage drop $R_s i_s$ small, the stator flux variation can be expressed as

$$\Delta\bar{\Phi}_s \cong \bar{v}_s \, \Delta t \quad (7)$$

Eq. 7 indicates that $\bar{\Phi}_s$ draws a locus which is determined by the selected voltage vector and the period Δt in which the voltage vector is applied to stator windings. It is then possible to drive $\bar{\Phi}_s$ along any prefixed track curve. In steady state conditions, for sinusoidal waveforms, the stator flux vector has to describe a circular locus. As it is shown in Fig. 2, $\Delta\bar{\Phi}_s$ can be resolved in two perpendicular components in the r-t reference frame rotating with $\bar{\Phi}_s$.

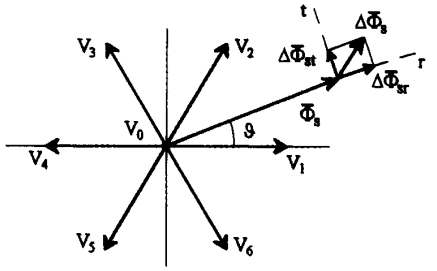

Fig. 2 - Radial and tangential components of the flux variation.

In order to control the stator flux magnitude it is opportune to select the voltage vector which determines a high radial component of $\Delta\bar{\Phi}_s$. In steady state conditions the stator and rotor flux vectors have the same angular speed and the angle θ_{sr} between these vectors determines the electromagnetic torque value, according to the following expression

$$T = P \frac{M}{\sigma L_s L_r} \Phi_s \Phi_r \sin\vartheta_{sr} \quad (8)$$

Any command which causes the flux angle to change will determine a torque variation. In order to control the torque it is then opportune to select the voltage vector which determines a high tangential component of $\Delta\bar{\Phi}_s$.

In these terms the flux and torque commands are not inherently decoupled as in traditional field oriented control. However, selecting the proper voltage vector in order to maintain Φ_s and T within the limits of two hysteresis bands results in a direct and decoupled control. At each sampling period one of the four possible combinations of torque and flux increase or decrease may be required (Tab. I). Many voltage selection strategies can be utilised as widely discussed in [7]. Each selection strategy affects the drive performance in terms of torque and current ripple, switching frequency and torque response. In this paper the attention is mainly focused on the influence of torque and stator flux band amplitudes on drive performance, then reference is made to the more usual selection strategy of Tab. I.

TAB. I - VOLTAGE VECTOR SELECTION STRATEGY.

	$\Phi_s \Uparrow$	$\Phi_s \Downarrow$
$T \Uparrow$	V_{k+1}	V_{k+2}
$T \Downarrow$	V_0	V_0

Assuming the stator flux lying in the k-th sector (k=1,2,..6) of the d-q plane, V_{k+1} or V_{k+2} can be selected in order to increase the torque, while zero voltage vector V_0 is utilised to decrease the torque.

DIGITAL IMPLEMENTATION

The DTC scheme requires as input variables the desired values of torque and flux and calculates, at each sampling period, the stator voltage required to drive the flux and torque to the reference values. Fig. 3 illustrates the computational flow of the implemented system. The DSP-based controller reads in the torque and flux references, the DC link voltage and two line currents at the beginning of each sampling period. Then the controller executes the A/D conversions, performs all the necessary computations and outputs the inverter switching state.

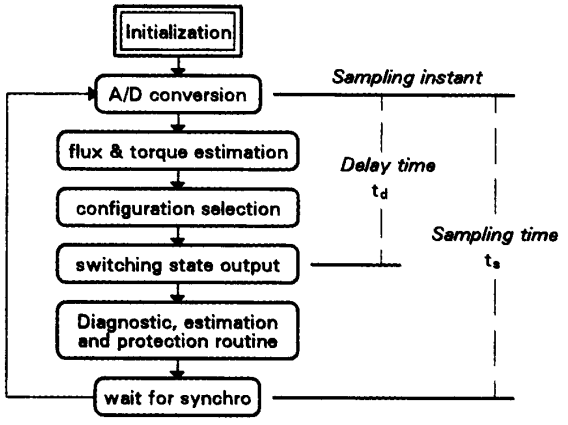

Fig. 3 - Flowchart of DTC scheme.

The DSP, even if characterised by multiplication capability and high

speed, needs a certain amount of time to execute the entire control algorithm. This time, together with the time required for overcurrent protection and diagnostic facility, determines the minimum value of the sampling period t_s. The control system acts on the stator voltage vector at each sampling period but, owing to the computational time required, a delay period t_d is present between the sampling instant and the inverter switches commutation. As with any predictive control scheme, this fact, combined with the performance of hysteresis band controllers, results in a mean delay period for the inverter commands equal to $t_d+t_s/2$. As a consequence the instantaneous values of stator flux magnitude and torque may exceed the upper and lower band limits of the prefixed hysteresis bands.

Of course, these phenomena are as much evident as the sampling period and the computational time increase. The overshoots are related to the rate of change of stator flux and torque, which in turn depends on the DC link voltage and the total leakage inductance.

From these considerations it appears evident that even with zero band amplitude, the stator flux and torque will be affected by a ripple.

Performance evaluation criteria

The drive performance obtained for different hysteresis band amplitudes have been compared in terms of torque dispersion, total current harmonic distortion, average inverter switching frequency and drive losses [8], [9].

According to the principle of operation of DTC, the torque presents a pulsation that is directly related to the amplitude of its hysteresis band. The torque pulsation is required to be as small as possible because it causes vibration and acoustic noise. In order to evaluate the torque pulsation it is opportune to introduce the dispersion of the torque δ which is defined as

$$\delta = \sqrt{\frac{1}{t_c}\int_0^{t_c}\left(\frac{T}{T_0}-1\right)^2 dt}$$

where

t_c = fundamental period

T = instantaneous torque value

T_0 = average torque value.

The amplitude of the flux hysteresis band directly affects the ripple of the stator flux. This in turn determines a corresponding distortion of the motor current with a close correlation to harmonic copper losses. The motor current waveforms and the corresponding harmonic spectra are important parameters to evaluate the drive performance. For this purpose the total harmonic distortion factor THD is considered, which is defined as

$$THD = \sqrt{\frac{\left(I^2 - I_1^2\right)}{I_1^2}}$$

where

I = rms value of the motor current

I_1 = rms value of the fundamental harmonic component.

The amplitude of the torque and flux hysteresis bands affects the inverter switching frequency and then the switching losses. The average inverter switching frequency f_s is defined as

$f_s = N_s / t_c$

where

N_s = number of switchings in one fundamental period.

Simulation Results

A computer model of the overall system has been developed to compare the drive performance as function of the hysteresis band amplitudes of stator flux and torque. The simulations were carried out so as to accurately predict the performance of the hardware controller. In particular, the performed calculations are done with the same precision in the software as they would be done in actual hardware.

The simulations have been performed for a standard 4 kW, 4-pole, 220 V, 50 Hz induction motor having the following parameters:

R_s= 1.1 Ω R_r= 1.05 Ω

L_s= 0.12 H L_r= 0.12 H M= 0.115 H

The numerical results have been obtained for ω_m=55 rad/s, T_0=26 Nm and Φ_0= 0.64 Wb.

Effects of flux hysteresis band amplitude

For a prefixed torque band amplitude ΔT, the inverter switching frequency is related to the amplitude of the flux hysteresis band $\Delta\Phi$. A small flux band amplitude determines higher switching frequency. The stator flux vector locus approaches a circle and the phase current waveform is nearly sinusoidal. These operating conditions determine low harmonic copper losses in the machine and high switching losses in the inverter. As the amplitude of the flux hysteresis band increases the switching frequency decreases and the stator flux vector locus degenerates to a hexagon. These operating conditions require the smallest number of commutations in each fundamental period, but determine harmonic distortion in phase current similar to six-step inverter-fed induction machine. As a consequence the commutation losses decrease while the harmonic copper losses increase.

As an example, some simulation results showing the stator flux vector loci and the phase current waveforms, for different values of the stator flux band amplitude, are given in Figs. 4, 5 and 6. These results have been obtained assuming $\Delta T/T_0$= 0.

For a detailed analysis of the above mentioned phenomena it is interesting to examine Figs. 7 and 8. Fig. 7 illustrates the variation of the total harmonic distortion factor as function of flux hysteresis band amplitude, for fixed torque hysteresis band amplitude. Similarly, Fig. 8 shows the variation of the average inverter switching frequency.

These results demonstrate that, for a prefixed torque hysteresis band amplitude, the current distortion increases with the flux hysteresis band amplitude. It should be noted that the percent increase is more appreciable with low values of torque band amplitude. Furthermore, as $\Delta\Phi$ is increased the average switching frequency shows a decline, as expected. An appreciable percent decrease of f_s appears for high values of ΔT. From these considerations, small flux hysteresis bands should be preferred when high-switching speed semiconductor devices are utilised because their switching losses are usually negligible with respect to on-state losses. In this way the output current harmonics can be strongly reduced.

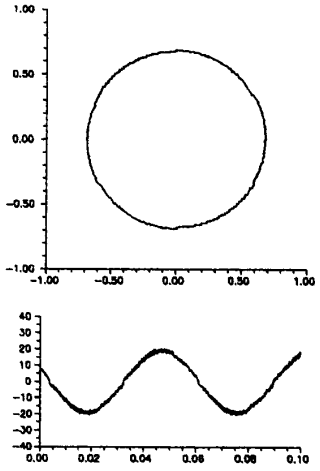

Fig. 4 - Stator flux vector locus and phase current waveform for $\Delta\Phi/\Phi_0$=0

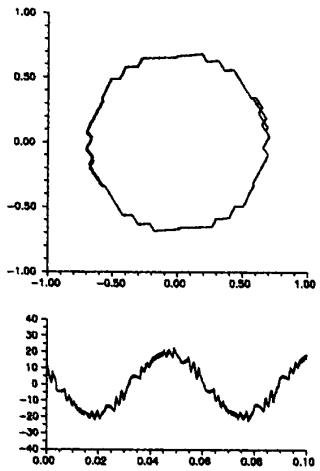

Fig. 5 - Stator flux vector locus and phase current waveform for $\Delta\Phi/\Phi_0$= 0.07

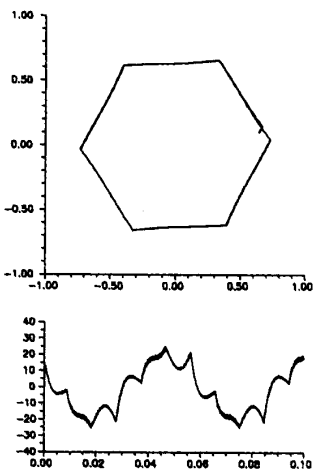

Fig. 6 - Stator flux vector locus and phase current waveform for $\Delta\Phi/\Phi_0$=0.14

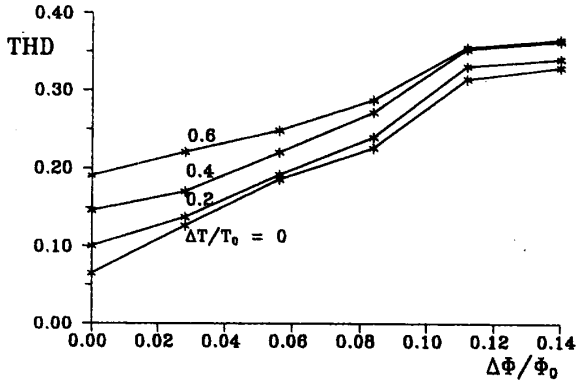

Fig. 7 - Total harmonic distortion factor as function of flux hysteresis band.

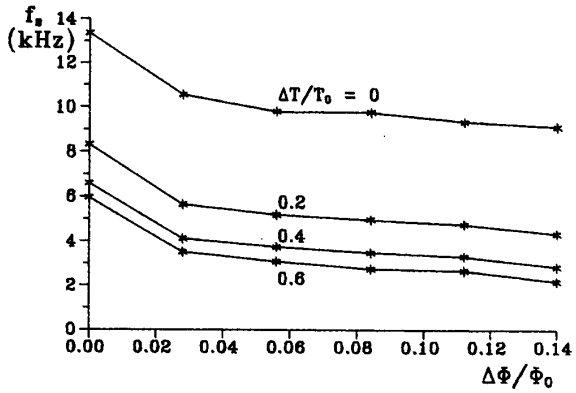

Fig. 8 - Average inverter switching frequency as function of flux hysteresis band.

In order to emphasise the correlation between harmonic copper losses and switching losses it is useful to analyse Fig. 9. This figure shows the relationship between THD^2 and f_s for various flux and torque hysteresis band amplitudes. Each curve is obtained for fixed ΔT. It is apparent that for each curve the increase of $\Delta\Phi$ is initially associated to a decrease of f_s, then to an increase of THD^2.

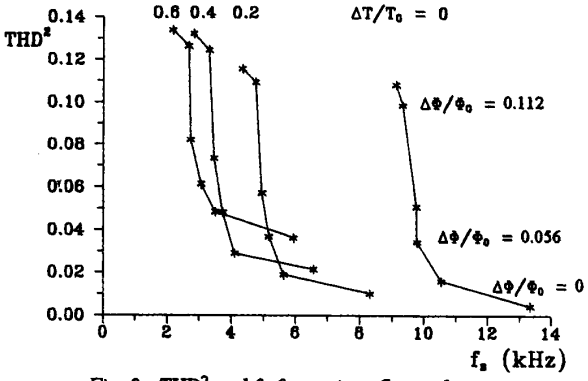

Fig. 9 - THD^2 and f_s for various flux and torque hysteresis band amplitudes.

Effects of torque hysteresis band amplitude

The effects of torque band amplitude on THD and f_s can be analysed utilising Figs. 7 and 8 again. In Fig. 7 it can be observed that ΔT mostly affects the total harmonic distortion factor for small values of $\Delta\Phi$. As $\Delta\Phi$ increases the harmonic current distortion approaches that of a six-step voltage operation and is moderately affected by ΔT. Furthermore, Fig. 8 shows that the average switching frequency is strongly affected by ΔT.

As previously described the pulsation of the torque is related to the amplitude of its hysteresis band. Fig. 10 shows that the dispersion of the torque δ varies practically linearly with ΔT. Owing to the effects due to the digital implementation, δ assumes a non null value for ΔT= 0.

The amplitude of $\Delta\Phi$ has practically no influence on δ and thus only one curve has been plotted ($\Delta\Phi/\Phi_0$ = 0.056).

The results obtained emphasise the importance of a careful choice of ΔT and $\Delta\Phi$. In particular, optimum drive performance in terms of

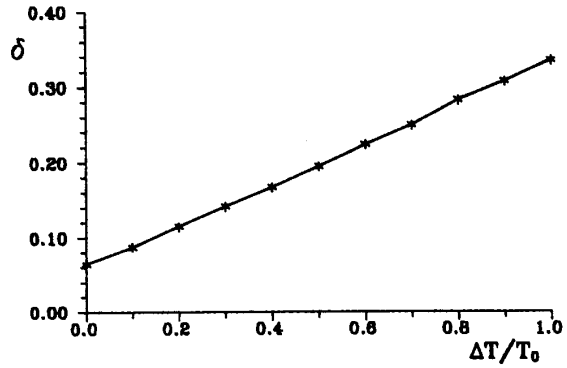

Fig. 10 - Dispersion of the torque as function of torque hysteresis band.

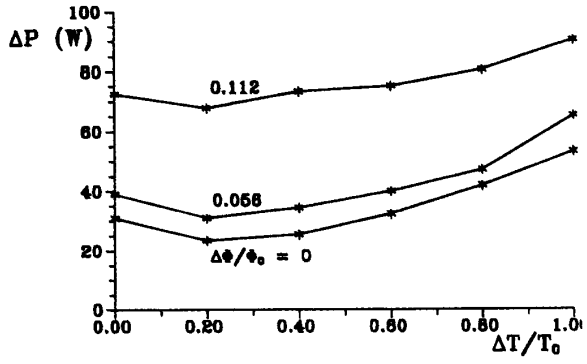

Fig. 11 - Sum of harmonic copper losses and switching losses as function of torque hysteresis band.

drive losses may be achieved taking into account that the harmonic copper losses are related to the squared THD and the switching losses to the average switching frequency of the inverter. In order to carry out a quantitative analysis it is necessary to know the motor parameters and the characteristics of the inverter high-power semiconductor devices.

Assuming for simplicity the rotor resistance constant and unaffected by frequency, the harmonic copper losses can be assumed proportional to THD^2. The switching losses are evaluated with reference to IGBT devices of the type described in the next section. Fig. 11 shows the sum of harmonic copper losses and switching losses as function of ΔT. Each curve is related to a fixed value of $\Delta\Phi$. For the drive system considered the losses assume a minimum value for $\Delta\Phi/\Phi_0 = 0$ and $\Delta T/T_0 = 0.2$.

Although the analysis carried out has general validity, the numerical results may be quite different according to motor parameter values and semiconductor device characteristics.

In this section the attention has been mainly focused on frequency and harmonic effects associated with different values of flux and torque band amplitudes, for a fixed speed of 55 rad/s. The numerical analysis has shown that the variation of THD with the mechanical speed ω_m can be neglected. The average switching frequency varies with ω_m showing higher values for ω_m ranging from 0.4 to 0.6 p.u. . However, these results doesn't influence the qualitative analysis earlier presented. The only effect is a slight change of the numerical values shown in Figs. 7, 8, 9, 10 and 11.

Experimental Results

An experimental drive system has been realised and tested using the direct torque control technique. The experimental set-up includes a fully digital controlled IGBT inverter and a 4 kW standard induction motor. The main switches are rated at 1000 V, 50 A.

For the realisation of the proposed control system, a DSP based

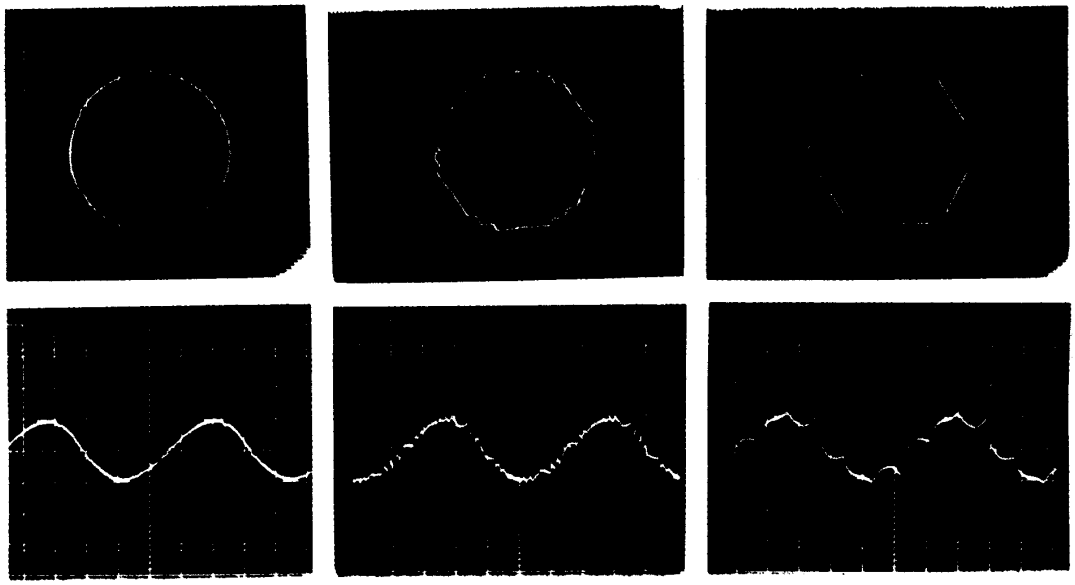

Fig. 12 - Stator flux vector locus and phase current waveform for $\Delta\Phi/\Phi_0=0$.

Fig. 13 - Stator flux vector locus and phase current waveform for $\Delta\Phi/\Phi_0= 0.07$.

Fig. 14 -Stator flux vector locus and phase current waveform for $\Delta\Phi/\Phi_0= 0.14$.

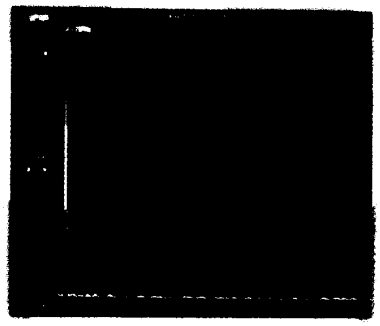

Fig. 15 - Measured stator current spectrum for $\Delta\Phi/\Phi_0 = 0$.

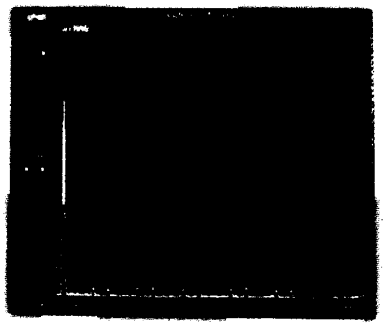

Fig. 16 - Measured stator current spectrum for $\Delta\Phi/\Phi_0 = 0.07$.

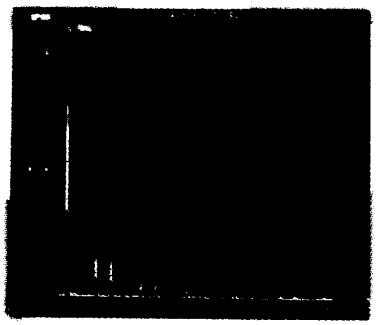

Fig. 17 - Measured stator current spectrum for $\Delta\Phi/\Phi_0 = 0.14$.

processing system has been chosen. It comprehends a 1 MHz, 8-channel 12-bit A/D converter, 2-channel 12-bit D/A converter and a 20 MHz TMS320E15 signal processor. The torque and flux reference values are read-in through two channels of the A/D converter. The quantities calculated by the digital controller can be selected and read-out through the D/A converters.

Figs. 12, 13 and 14 show the experimental results obtained for the same operating conditions as in Figs. 4, 5 and 6 respectively. As it is possible to see there is a good correlation between the experimental and simulation results. The corresponding measured current harmonic spectra are shown in Figs. 15, 16 and 17. Fig. 17 clearly shows the presence of the low order harmonics typical of six-step behaviour ($n = 6k \pm 1$, $k = 1,2,3,...$). Reducing the flux hysteresis band results in a smoothed and right-shifted harmonic distribution.

Conclusions

In this paper a control scheme for direct torque control of induction machine has been analysed in order to emphasise the effects of flux and torque hysteresis band amplitudes on drive performance. For the comparative analysis some performance evaluation criteria such as torque dispersion, harmonic distortion factor, average switching frequency and drive losses have been utilised. The results obtained show that the flux hysteresis band mainly affects the motor current distortion in terms of low order harmonics. In particular, high values of the flux hysteresis band determine high harmonic copper losses. The switching frequency and then the switching losses are mainly affected by the torque hysteresis band. It has been shown that a minimum for the sum of the harmonic copper losses and switching losses may be determined. When the torque hysteresis band amplitude is established by load requirements, the drive losses are function of $\Delta\Phi$ only. For the drive system considered in this paper, the drive losses assume the lower values for $\Delta\Phi = 0$. However, considering different semiconductor devices or motors, the lower values of the drive losses may occur for $\Delta\Phi$ values greater than zero.

References

[1] I. Takahashi, T. Noguchi: *A new quick-response and high-efficiency control strategy of an induction motor.* IEEE Trans. on IA, Vol. IA-22, N. 5, Sept/Oct 1986, pp 820-827

[2] I. Takahashi, T. Kanmachi: *Ultra-wide speed control with a quick torque response AC servo by a DSP.* Proc. EPE, Firenze (I), September, 3-6 1991, Proc. Vol. III, pp. 572 - 577.

[3] M. Depenbrok: *Direct Self-Control (DSC) of Inverter-Fed Induction Machine.* IEEE Trans. on PE, Vol. PE-3, N. 4, Oct. 1988, pp. 420-429.

[4] U. Baader, M. Depenbrok: *Direct Self Control (DSC) of Inverter-Fed Induction Machine: A Basis for Speed Control Without Speed Measurement.* IEEE Trans. on IA, Vol. IA-28, N. 3, May/June 1992, pp. 581-588.

[5] D. Casadei, G. Grandi, G. Serra: *Study and implementation of a simplified and efficient digital vector controller for induction motors.* IEE Conf. Pub. No 376, Proc. EMD, Oxford (UK), 8-10 September 1993, pp. 196-201.

[6] D. Casadei, G. Grandi, G. Serra: *Rotor flux oriented torque-control of induction machines based on stator flux vector control.* IEE Conf. Pub. No 377, Proc. EPE, Brighton (UK), 13-16 September 1993, Vol. 5, pp. 67-72.

[7] D. Casadei, G. Grandi, G. Serra, A. Tani: *Switching strategies in direct torque control of induction machines.* Proc. ICEM, Paris (F), 5-8 September 1994.

[8] Y. Iwaji, S. Fukuda: *A PWM control method using pulse frequency modulation technique.* Proc. EPE, Firenze (I), 3-6 September 1991, Vol. II, pp. 76-82.

[9] A. Tripathi, P. C. Sen: *Comparative analysis of fixed and sinusoidal band hysteresis current controllers for voltage source inverters.* IEEE Trans. on IE, Vol. 39, N. 1, Feb 1992, pp. 63-73.